

Dispersive destabilization of nonlinear light propagation in fiber Bragg gratings: a numerical verification

Carlos Martel* and Carlos M. Casas

Depto. de Fundamentos Matemáticos,

E.T.S.I. Aeronáuticos, Universidad Politécnica de Madrid,

Plaza Cardenal Cisneros 3, 28040 Madrid, Spain

Abstract

This paper presents some numerical simulations of the full one-dimensional Maxwell-Lorentz equations that describe light propagation in fiber Bragg gratings in order to confirm that the standard nonlinear coupled mode equations fail to predict the weakly nonlinear dynamics of the system when dispersive instabilities come into play, and that, in this case, the correct slow envelope description of the system requires to consider higher order dispersion effects.

arXiv:nlin/0702012v1 [nlin.PS] 7 Feb 2007

*Electronic address: martel@fmetsia.upm.es

I. INTRODUCTION

The nonlinear coupled mode equations (NLCME) are the envelope equations currently used to study the weakly nonlinear dynamics of light propagation in fiber Bragg gratings. These equations do not include dispersion effects. In this paper we integrate numerically the full 1D Maxwell-Lorentz equations in a fiber grating in order to show that the dispersion effects can be essential in the dynamics of the system and that the correct weakly nonlinear description of the system has necessarily to include higher order dispersion terms. The resulting envelope equations are asymptotically nonuniform in the sense that they include terms with different asymptotic order, and this is a standard situation for general extended, propagative (i.e., with order one group velocity) pattern forming systems.

The weakly nonlinear dynamics of resonant light propagation in a Fiber Bragg grating (FBG), i.e., optical fiber with a periodic variation of the refractive index along its length, is usually described using the so-called nonlinear coupled mode equations (NLCME)

$$A_t^+ = A_x^+ + i\kappa A^- + iA^+(\sigma|A^+|^2 + |A^-|^2), \quad (1)$$

$$A_t^- = -A_x^- + i\kappa A^+ + iA^-(\sigma|A^-|^2 + |A^+|^2), \quad (2)$$

which prescribe the evolution of the complex envelopes A^\pm of the two slowly modulated resonant wavetrains that approximately constitute the actual field inside the FBG

$$E \sim A^+(x, t) e^{ix+i\omega t} + A^-(x, t) e^{-ix+i\omega t} + \text{c.c.} + \dots, \quad (3)$$

see e.g. [1, 2, 3, 4, 5]. The NLCME above, where space, time and the amplitudes have been rescaled to reduce the number of parameters, retain the combined effect of the group velocity, the coupling induced by the grating and the weakly nonlinear interaction of the wavetrains. This formulation, apart from FBG, has been also used to describe the evolution of quasi-onedimensional Bose-Einstein condensates in optical lattices [6, 7] and, in general, the NLCME are commonly regarded as the normal form for the weakly nonlinear dynamics of any extended, propagative system without dissipation and with a weak spatial periodic structure.

In a recent paper [8] one of the authors showed that the NLCME (1)-(2) fail to predict the dynamics of the system when dispersive instabilities (that cannot be detected using the NLCME formulation) come into play, and that, for both signs of the dispersion coefficient, there are always stable solutions according to the NLCME that are dispersively unstable. In order to correctly

describe the weakly nonlinear evolution of the system, the effect of higher order dispersion has to be retained and the appropriate amplitude equations are the following dispersive nonlinear coupled mode equations (NLCMED)

$$A_t^+ = A_x^+ + i\kappa A^- + iA^+(\sigma|A^+|^2 + |A^-|^2) + i\varepsilon A_{xx}^+, \quad (4)$$

$$A_t^- = -A_x^- + i\kappa A^+ + iA^-(\sigma|A^-|^2 + |A^+|^2) + i\varepsilon A_{xx}^-. \quad (5)$$

This dispersive system was introduced and analyzed in detail in [8], but we think it is convenient to briefly remind here some of the results obtained in that paper:

1. The scaling of the NLCMED is the same of the NLCME: the characteristic length scale is the slow scale that results from the balance of the advection term with the small effect of the grating, the characteristic time is the corresponding transport time scale and the characteristic size of the wavetrains results from the saturation of the small nonlinear terms. The small amplitude slow envelope assumption, which is the key assumption that allow us to derive both systems of equations, forces the dispersive terms to be always small as compared with the advection terms (in other words, the nonzero group velocity turns this system into a transport dominated one) and therefore (with the scaling mentioned above) the NLCMED must be considered only in the physically relevant regime $\varepsilon \rightarrow 0$.
2. The NLCMED are asymptotically nonuniform, in the sense that the resulting asymptotic model, in the $\varepsilon \rightarrow 0$ limit, still contains the small parameter ε . This is due to the fact that the NLCMED include simultaneously two balances with different asymptotic order: one induced by the dominant transport terms and the other associated with the underlying effect of dispersion. This kind of asymptotically nonuniform amplitude equations have been previously derived in the context of water waves [9] and for the onset of the oscillatory instability in spatially extended dissipative systems [10, 11].
3. Two spatial scales are present in the NLCMED: transport scales $\delta x_{\text{trans}} \sim 1$, and dispersive scales $\delta x_{\text{disp}} \sim \sqrt{|\varepsilon|} \ll 1$. The dispersive scales are small as compared with the transport scales but still large as compared with the wavelength of the basic resonant wavetrains in expression (3), which, in the scaling we are using, is of the order of $|\varepsilon| \ll 1$, and therefore the slow envelope assumption is not violated.

4. If only transport scales are present, then the dispersion terms in the NLCME $|\varepsilon A_{xx}|, |\varepsilon B_{xx}| \sim |\varepsilon| \ll 1$ can be safely neglected (they produce only a small quantitative correction that vanishes as $\varepsilon \rightarrow 0$) and the evolution of the system is well represented by the NLCME. On the other hand, if the small dispersive scales do develop, then the NLCME do not correctly predict the dynamics system and the NLCMEd must be used instead. The onset of the dispersive scales is not a higher order, longer time effect; it takes place in the same timescale of the NLCME no matter how small the dispersion coefficient ε is. Once the dispersive scales appear they typically spread all over the domain giving rise to very complicated spatio-temporal dynamics. This dispersive destabilization can be simply regarded as the standard modulational instability of the NLS-like dynamics that lays beneath the dominant transport induced dynamics.
5. The stability of the family of uniform modulus solutions, known as continuous waves (CW), is drastically affected by dispersion. The stability predictions for the CW from the NLCME differ completely from those obtained from the NLCMEd for both signs of the dispersion coefficient ε , no matter how small it may be.

Despite of the results presented in [8] it appears that the NLCME continue to be used as the amplitude equations for the description of light propagation in FBG and for the weakly nonlinear dynamics of BEC in optical lattices without paying any attention to the effect of dispersion. In order to make clear that the correct amplitude equations are the NLCMEd, we have decided to carry out some numerical integrations of the full 1D Maxwell-Lorenz equations (MLE) in a long fiber Bragg grating and check that the stability predictions for the CW given by the NLCME are wrong and that the dispersive NLCMEd give the correct results.

This paper is organized as follows: in the following section we derive the explicit expressions of the coefficients of the NLCMEd from the MLE and, in the next and final section of this paper, we present some numerical integrations of the MLE starting from a perturbed CW and compare them with the CW stability characteristics predicted by the NLCME and the NLCMEd.

II. NLCMED DERIVATION FROM THE MLE

Our formulation follows closely that of ref. [5]. We have decided to include here a quited detailed derivation of the NLCMEd from the MLE because we use rather new derivation procedure

that has the advantage of not requiring to assume any a priori relation among the different small parameters of the problem.

We describe the propagation of light in a fiber with a periodic grating and a cubic nonlinearity using the one-dimensional Maxwell's equations [12, 13] for the evolution of the electromagnetic fields together with an anharmonic Lorentz oscillator model for the polarization (see e.g. [5, 14] and references therein)

$$\frac{\partial B}{\partial t} = \frac{\partial E}{\partial x}, \quad (6)$$

$$\mu_0 \frac{\partial D}{\partial t} = \frac{\partial B}{\partial x}, \quad (7)$$

$$D = \epsilon_0 E + P, \quad (8)$$

$$\Omega_p^{-2} \frac{\partial^2 P}{\partial t^2} + (1 - 2\Delta n \cos(2\pi x/\lambda_g))P - \gamma P^3 = \epsilon_0 \chi E. \quad (9)$$

In the system above, the electric field E , the magnetic field B , the dielectric displacement D and the polarization P are scalar fields that depend on the spatial variable x and on time t . μ_0 and ϵ_0 denote, respectively, the permeability and the permittivity of the vacuum. The characteristic frequency Ω_p accounts for the non instantaneous polarization response of the media, Δn and λ_g represent the strength and the period of the grating, that is, the strength and the period of the spatial periodic variation of the refractive index of the fiber (Δn measures the size of the nonuniformities of the refraction index relative to its mean value n_0 , see Fig. 1), χ is the linear polarizability of the medium ($n_0^2 = 1 + \chi$) and $\gamma > 0$ is the coefficient of the nonlinear Kerr effect.

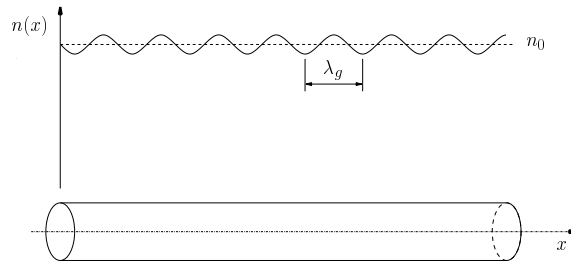


Figure 1: One dimensional fiber with a periodic variation of the refractive index.

In order to simplify subsequent calculations it is convenient to make the system (6)-(9) nondimensional using the following rescalings:

$$B = \sqrt{\mu_0/(\epsilon_0\gamma)}\tilde{B}, \quad D = (1/\sqrt{\gamma})\tilde{D}, \quad E = (1/\sqrt{(\epsilon_0\gamma)})\tilde{E}, \quad P = (1/\sqrt{\gamma})\tilde{P},$$

$$x = (\lambda_g/\pi)\tilde{x}, \quad t = (\lambda_g/c\pi)\tilde{t},$$

where $c^2 = 1/(\epsilon_0\mu_0)$ is the vacuum speed of light. After dropping tildes and eliminating D and B , the nondimensional MLE can be written in the form

$$\frac{\partial^2(E+P)}{\partial t^2} = \frac{\partial^2 E}{\partial x^2}, \quad (10)$$

$$\frac{\partial^2 P}{\partial t^2} = -\omega_p^2(1 - 2\Delta n \cos(2x))P + \omega_p^2(n_0^2 - 1)E + \omega_p^2 P^3. \quad (11)$$

where the grating period is now equal to π and the dimensionless finite time polarization response frequency is given by $\omega_p^2 = \Omega_p^2 \lambda_g^2 / (c^2 \pi^2)$.

In the absence of grating, the linear propagation characteristics of a wavetrain of the form

$$\begin{pmatrix} E(x, t) \\ P(x, t) \end{pmatrix} = \begin{pmatrix} E_k \\ P_k \end{pmatrix} e^{ikx + i\omega_k t} + \text{c.c.}, \quad (12)$$

are given by the following dispersion relation

$$\omega_k^4 - \omega_k^2(k^2 + \omega_p^2 n_0^2) + \omega_p^2 k^2 = 0, \quad (13)$$

which, for $n_0^2 > 1$, has four real roots of the form

$$\omega_k = \pm \sqrt{(k^2 + \omega_p^2 n_0^2)/2 \pm \sqrt{(k^2 + \omega_p^2 n_0^2)^2/4 - \omega_p^2 k^2}}, \quad (14)$$

and associated eigenvectors

$$\begin{pmatrix} E_k \\ P_k \end{pmatrix} = \begin{pmatrix} \omega_k^2 \\ k^2 - \omega_k^2 \end{pmatrix}. \quad (15)$$

The four branches of the dispersion relation (14) are plotted in Fig. 2. There are two different behaviors for large wavenumbers: one is dominated by the finite time polarization response of the medium, $\omega_k \rightarrow \pm\omega_p$ as $k \rightarrow \pm\infty$, and the other, $\omega_k \rightarrow \pm k$ as $k \rightarrow \pm\infty$, corresponds to propagation like in the vacuum, without polarization effects.

The small nonuniformities of the refractive index, $\Delta n \ll 1$, and the effect of the small nonlinearity can be accounted for by allowing the wavetrains that resonate with the grating to be slowly modulated in space and time

$$\begin{pmatrix} E(x, t) \\ P(x, t) \end{pmatrix} = V_0(A^+(x, t)e^{ix+i\omega t} + A^-(x, t)e^{-ix+i\omega t}) + \text{c.c.} + \dots, \quad (16)$$

where

$$V_0 = \begin{pmatrix} \omega^2 \\ 1 - \omega^2 \end{pmatrix}, \quad \text{and} \quad \omega = \sqrt{(1 + \omega_p^2 n_0^2)/2 \pm \sqrt{(1 + \omega_p^2 n_0^2)^2/4 - \omega_p^2}}, \quad (17)$$

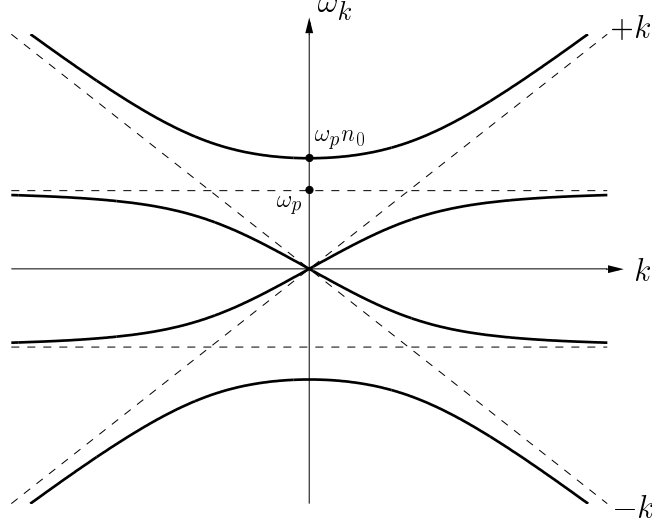


Figure 2: Sketch of the dispersion relation (14).

and the weakly nonlinear level of this approach requires essentially that

$$\dots \ll |A_{xx}^\pm| \ll |A_x^\pm| \ll |A^\pm| \ll 1, \quad \dots \ll |A_t^\pm| \ll |A^\pm| \ll 1 \quad \text{and} \quad \Delta n \ll 1, \quad (18)$$

that is, small amplitudes that depend slowly on space and time and small grating strength. The solution of eqs. (10)-(11) and the amplitude equations can be expanded in powers of the small quantities Δn , A^\pm , A_x^\pm , A_{xx}^\pm, \dots as

$$\begin{aligned} \left\{ \begin{array}{l} E(x, t) \\ P(x, t) \end{array} \right\} &= V_0(A^+ e^{ix+i\omega t} + A^- e^{-ix+i\omega t}) + \text{c.c.} + \\ &+ v_1^+ A_x^+ + v_1^- A_x^- + v_2^+ A_{xx}^+ + v_2^- A_{xx}^- + \dots, \end{aligned} \quad (19)$$

$$A_t^+ = \alpha_0^+ A^+ + \alpha_1^+ A_x^+ + \alpha_2^+ A_{xx}^+ + \dots, \quad (20)$$

$$A_t^- = \alpha_0^- A^- + \alpha_1^- A_x^- + \alpha_2^- A_{xx}^- + \dots, \quad (21)$$

which, once inserted into eqs. (10)-(11), provide a linear nonhomogeneous system for the contribution of each order. For the resonant terms, i.e., those proportional to $e^{\pm ix \pm i\omega t}$, a condition must be satisfied to ensure that there are not secular terms in the short time scale. In other words, the linear problems corresponding to the resonant terms are singular and hence a solvability condition must be satisfied by the nonhomogeneous part; these solvability conditions yield the coefficients of the amplitude equations.

Notice that only the resonant terms contribute to the amplitude equations and only the amplitude equation for A^+ has to be calculated because the corresponding equation for A^- can be obtained

by simply applying the symmetry

$$x \rightarrow -x \quad A^+ \longleftrightarrow A^-, \quad (22)$$

which comes from the spatial reflection symmetry of the original problem (10)-(11).

The linear terms in the amplitude equations can be easily anticipated because they correspond to the Taylor expansion of the dispersion relation (14) at $k = 1$ (see e.g. [15]),

$$i(\omega_k|_{k=1} - \omega)A^+ + \left. \frac{d\omega_k}{dk} \right|_{k=1} A_x^+ - i\frac{1}{2} \left. \frac{d^2\omega_k}{dk^2} \right|_{k=1} A_{xx}^+ + \dots$$

The first coefficient obviously vanishes (see eq. (17)) and the second and third coefficients are, respectively, the group velocity and the higher order dispersion, which, after making use of eq. (13), can be written as

$$v_g = \left. \frac{d\omega_k}{dk} \right|_{k=1} = \frac{\omega(\omega^2 - \omega_p^2)}{\omega^4 - \omega_p^2}, \quad (23)$$

$$id = -i\frac{1}{2} \left. \frac{d^2\omega_k}{dk^2} \right|_{k=1} = -i\frac{1}{2} \frac{\omega^3(\omega^2 - 1)(\omega^2 - \omega_p^2)(3\omega_p^2 + \omega^4)}{(\omega^4 - \omega_p^2)^3}, \quad (24)$$

which correspond to the group velocity and dispersion of the fiber without grating.

The first order, resonant contributions of the grating to the expansion of the solution (16) and to the amplitude equation (20) are of the form

$$W\Delta n A^- e^{ix+i\omega t} \quad \text{and} \quad w\Delta n A^-,$$

where the two component vector W is given by the following linear, singular nonhomogeneous problem

$$\begin{bmatrix} \omega^2 - 1 & \omega^2 \\ (n_0^2 - 1)\omega_p^2 & \omega^2 - \omega_p^2 \end{bmatrix} W = -\omega_p^2 \begin{bmatrix} 0 & 0 \\ 0 & 1 \end{bmatrix} V_0 + 2i\omega w \begin{bmatrix} 1 & 1 \\ 0 & 1 \end{bmatrix} V_0.$$

This system can be solved only if the right hand side is orthogonal to the solution of the adjoint problem

$$V_0^a = \left\{ \begin{array}{c} \omega_p^2 - \omega^2 \\ \omega^2 \end{array} \right\},$$

and this solvability condition gives the value of the coefficient of the amplitude equation

$$w = i \frac{\omega(1 - \omega^2)}{2(\omega^4 - \omega_p^2)} \omega_p^2. \quad (25)$$

The first order contributions of the nonlinear term,

$$U_1 A^+ |A^+|^2 e^{ix+i\omega t}, \quad U_2 A^+ |A^-|^2 e^{ix+i\omega t} \quad \text{and} \quad u_1 A^+ |A^+|^2, \quad u_2 A^+ |A^-|^2,$$

are computed similarly: the following linear problems are obtained for the vectors U_1 and U_2

$$\begin{aligned} \begin{bmatrix} \omega^2 - 1 & \omega^2 \\ (n_0^2 - 1)\omega_p^2 & \omega^2 - \omega_p^2 \end{bmatrix} U_1 &= -3\omega_p^2 \begin{bmatrix} 0 \\ (1 - \omega^2)^3 \end{bmatrix} + 2i\omega u_1 \begin{bmatrix} 1 & 1 \\ 0 & 1 \end{bmatrix} V_0, \\ \begin{bmatrix} \omega^2 - 1 & \omega^2 \\ (n_0^2 - 1)\omega_p^2 & \omega^2 - \omega_p^2 \end{bmatrix} U_2 &= -6\omega_p^2 \begin{bmatrix} 0 \\ (1 - \omega^2)^3 \end{bmatrix} + 2i\omega u_2 \begin{bmatrix} 1 & 1 \\ 0 & 1 \end{bmatrix} V_0, \end{aligned}$$

and, after applying the solvability condition, the resulting amplitude equation coefficients are given by

$$u_1 = i \frac{3\omega(1 - \omega^2)^3}{2(\omega^4 - \omega_p^2)} \omega_p^2 \quad \text{and} \quad u_2 = i \frac{3\omega(1 - \omega^2)^3}{(\omega^4 - \omega_p^2)} \omega_p^2. \quad (26)$$

The ratio $u_2 = 2u_1$ could have been advanced; it is a well known result of the cubic nonlinearity of the problem [15].

Collecting the coefficients above (23)-(26) and applying the spatial reflection symmetry (22) the resulting amplitude equations can be written as

$$A_t^+ = v_g A_x^+ + idA_{xx}^+ + w\Delta n A^- + A^+(u_1|A^+|^2 + u_2|A^-|^2) + \dots, \quad (27)$$

$$A_t^- = -v_g A_x^- + idA_{xx}^- + w\Delta n A^+ + A^-(u_1|A^-|^2 + u_2|A^+|^2) + \dots \quad (28)$$

It is important to emphasize that no particular scaling among the small size of the amplitudes, the small grating depth, the slow time and the large spatial scale has been used; only the slow envelope, weakly nonlinear assumption expressed in (18) is actually required to obtain the above amplitude equations.

We will consider the simplest possible geometrical configuration: propagation of light in a fiber ring with length $L \gg 1$. The spatial periodicity condition implies that the boundary conditions for A^+ and A^- are (see eq. (16))

$$A^+(x + L)e^{i\theta} = A^+(x, t), \quad A^-(x + L)e^{-i\theta} = A^-(x, t). \quad (29)$$

Here $\theta = L \pmod{2\pi}$ measures the mismatch between the natural wavelength of the resonant wavetrains ($=2\pi$) and the period of the domain, but we will confine ourselves to the particular case $\theta = 0$, i.e., ring length equals to an integer multiple of the period of the wavetrains.

There are two possible choices ω^\pm depending on the sign selected in (17), see Fig. 3. The group velocity (23) is positive in both cases (it is the slope of the curve ω_k at $k = 1$ in Fig. 3), but the sign of the dispersion coefficient d (24), which is related to the curvature of the curve ω_k in Fig. 3, changes. On the other hand, the nonlinear and grating terms have imaginary parts that are always

negative; see eqs. (25) and (26) and Fig. 3, and recall that, using the dispersion relation eq. (13) for $k = 1$, the denominator can be written as $\omega^4 - \omega_p^2 = \omega^2[(\omega^2 - 1) + (\omega^2 - \omega_p^2 n_0^2)]$.

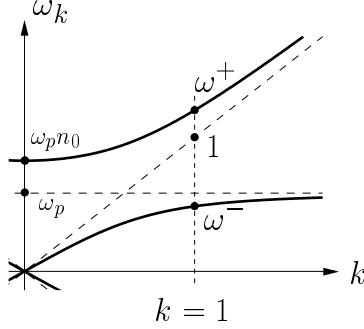


Figure 3: Detail of the dispersion relation (14) with the two frequencies ω^\pm for $k = 1$.

In order to make the nonlinear and grating coefficients positive, we will work with the complex conjugates of the amplitudes and, to absorb some parameters of the problem, we will also perform the following rescalings

$$x = L\tilde{x}, \quad t = (L/v_g)\tilde{t}, \quad \overline{A^\pm} = \sqrt{v_g/(L|u_2|)}\tilde{A}^\pm, \quad (30)$$

that, after dropping tildes, yield the scaled NLCMED

$$A_t^+ = A_x^+ + i\varepsilon A_{xx}^+ + i\kappa A^- + iA^+(\sigma|A^+|^2 + |A^-|^2), \quad (31)$$

$$A_t^- = -A_x^- + i\varepsilon A_{xx}^- + i\kappa A^+ + iA^-(\sigma|A^-|^2 + |A^+|^2), \quad (32)$$

$$A^\pm(x+1, t) = A^\pm(x, t), \quad (33)$$

where $\varepsilon = -d/(Lv_g) \ll 1$ is positive (negative) for $\omega = \omega^+$ ($\omega = \omega^-$), the scaled grating strength $\kappa = \Delta n L |w| / v_g \sim 1$ is always positive, and the nonlinear coefficient $\sigma = \frac{1}{2}$ (the standard NLCME are obtained by just by setting $\varepsilon = 0$ in the system above).

III. NUMERICAL RESULTS

In order to confirm that the correct stability predictions for the MLE are those given by the NLCMED, we numerically integrate the complete MLE (10)-(11) in a large ring shaped fiber grating, that is, with periodic boundary conditions,

$$E(x+L, t) = E(x, t), \quad P(x+L, t) = P(x, t),$$

and $L \gg 1$. The MLE are integrated numerically as a system of four first order equations, using Fourier series in space and a 4th order Runge-Kutta scheme [16] for the time integration of the resulting ODEs. The linear diagonal terms are integrated implicitly and the nonlinear terms are computed in physical space using the 2/3 rule to remove the aliasing terms [17]. The number of modes used in the simulations presented is $M_{\text{Fourier}} = 1024$ and the time step $\Delta t = .01$, and the Fourier transforms were performed using the FFTW routines [18].

The initial condition for all simulations is a CW

$$A_{\text{cw}}^+ = \rho \cos \theta e^{i\alpha t + imx}, \quad A_{\text{cw}}^- = \rho \sin \theta e^{i\alpha t + imx},$$

$$\alpha = \frac{\kappa}{\sin 2\theta} + \frac{1 + \sigma}{2} \rho, \quad m = \left(\frac{\kappa}{\sin 2\theta} + \frac{1 - \sigma}{2} \rho^2 \right) \cos 2\theta,$$

where $\rho > 0$ is the light intensity in the fiber and $\theta \in]-\frac{\pi}{2}, 0[\cup]0, \frac{\pi}{2}[$ measures the ratio between the two counterpropagating wavetrains (see [8]), with a small superimposed perturbation. Once a CW has been selected (κ , ρ and θ fixed) and the three MLE parameters ω_p^2 , n_0^2 and L are prescribed, the initial condition for the MLE is obtained from

$$\begin{Bmatrix} E \\ P \end{Bmatrix} = \begin{Bmatrix} \omega^2 \\ 1 - \omega^2 \end{Bmatrix} \sqrt{\frac{v_g}{L|u_2|}} (\bar{A}^+ e^{ix+i\omega t} + \bar{A}^- e^{-ix+i\omega t}) + \text{c.c.} + \dots, \quad (34)$$

and the remaining MLE coefficient, Δn , and the dispersion coefficient of the NLCMEd, ε , are given by

$$\Delta n = \frac{v_g}{L|w|} \kappa \quad \text{and} \quad \varepsilon = -\frac{d}{Lv_g}, \quad (35)$$

which can be computed after making use of (17), (23), (24), (25) and (26).

We consider only two configurations because the MLE numerical integrations are rather CPU costly (large system length and very long final integration time).

CASE 1 The initial CW parameters are $\kappa = 1$, $\theta = -\frac{\pi}{4}$ and $\rho^2 = 1$. The NLCMEd results presented in ref. [8] indicate that this CW is stable for negative dispersion and dispersively unstable for positive dispersion, while, according to the NLCME, this CW is always stable. The numerical integrations of the MLE presented in Fig. 4 correspond to the parameters $\omega_p^2 = 1$, $n_0^2 = 2$, $L = 128\pi$ (i.e., there are 128 grating oscillations inside the fiber ring). The first and second plot correspond, respectively, to $\omega = \omega^-$ and $\omega = \omega^+$ (that is, to negative and positive ε in the NLCMEd (see eq (35) and Fig.. 3)) with the MLE grating strength, Δn , that results from eq. (35). They show the time evolution of the spatial norm of the electric field,

$$\|E\| = \sqrt{\frac{1}{L} \int_0^L |E|^2 dx},$$

and look like a solid black patch due to the fact that $\|E\|$ oscillates very fast in time. In agreement with the NLCMEd predictions, the CW is stable for negative dispersion (first plot in Fig. 4) and unstable for positive dispersion (the instability growth can be appreciated from $t = 60000$ on in the second plot of Fig. 4). The corresponding spatial profiles of E at $t = 75000$ are given in the third and fourth plots of Fig. 4; for negative dispersion (third plot) a perfectly uniform amplitude oscillatory pattern is obtained (the CW pattern) but, for positive dispersion, a modulation is clearly present (fourth plot). In order to be sure that this is a dispersive instability we have repeated the unstable MLE simulation in a four times longer domain ($L = 256(2\pi)$). The resulting spatial profile of E at $t = 160000$ is shown in the last plot of Fig. 4. Notice how the number of basic wavelengths is now four times higher but the number of wavelengths of the modulation only approximately doubles (increases from 5 to 9), confirming the dispersive character of the instability whose characteristic size scale as \sqrt{L} (see ref. [8]).

CASE 2 The CW parameters are now $\kappa = 1$, $\theta = \frac{\pi}{4}$ and $\rho^2 = 1$, and the MLE parameters are the same as in the above case: $\omega_p^2 = 1$, $n_0^2 = 2$ and $L = 128\pi$. The first and third plot of Fig. 5 correspond to positive dispersion and indicate that the CW is now stable. The dispersion is negative in the second and fourth plot where the destabilization of the CW can be clearly seen both in the time evolution of $\|E\|$ and in the dispersive modulations that the spatial profile of E displays. This is again in perfect agreement with the linear stability results obtained from the NLCMEd [8] (the NLCME again wrongly labeled this CW as always stable).

In conclusion, the numerical simulations of the MLE indicate that the NLCME fail to describe the system evolution if dispersive instabilities (that cannot be detected using the NLCME formulation) come into play. In this case the higher order dispersion effects must be taken into account, and the amplitude equations that do correctly predict the weakly nonlinear dynamics of light propagation in FBG are the asymptotically nonuniform NLCMEd (4)-(5).

Acknowledgments

This work has been supported by the European Office of Aerospace Research and Development (FA8655-02-M4087), by the Spanish Dirección General de Investigación (MTM2004-03808) and

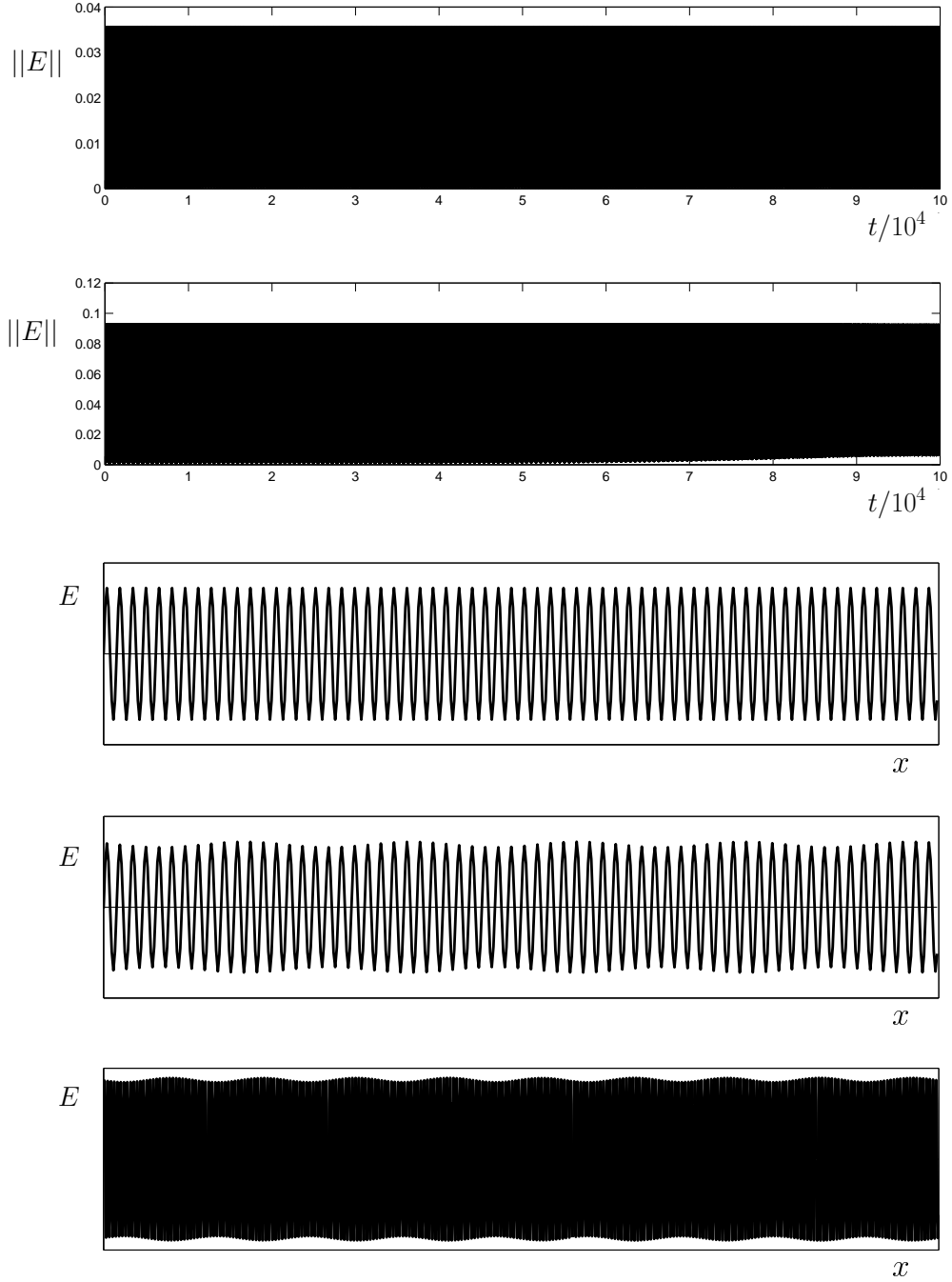


Figure 4: MLE simulation results starting from a CW ($\kappa = 1, \theta = -\frac{\pi}{4}$ and $\rho^2 = 1$) with a 10^{-4} perturbation. From top to bottom: time evolution of the spatial norm of E for ω^- and ω^+ , spatial profiles of E at $t = 75000$ for ω^- and ω^+ , and spatial profile of E at $t = 160000$ for ω^+ and $L = 512\pi$.

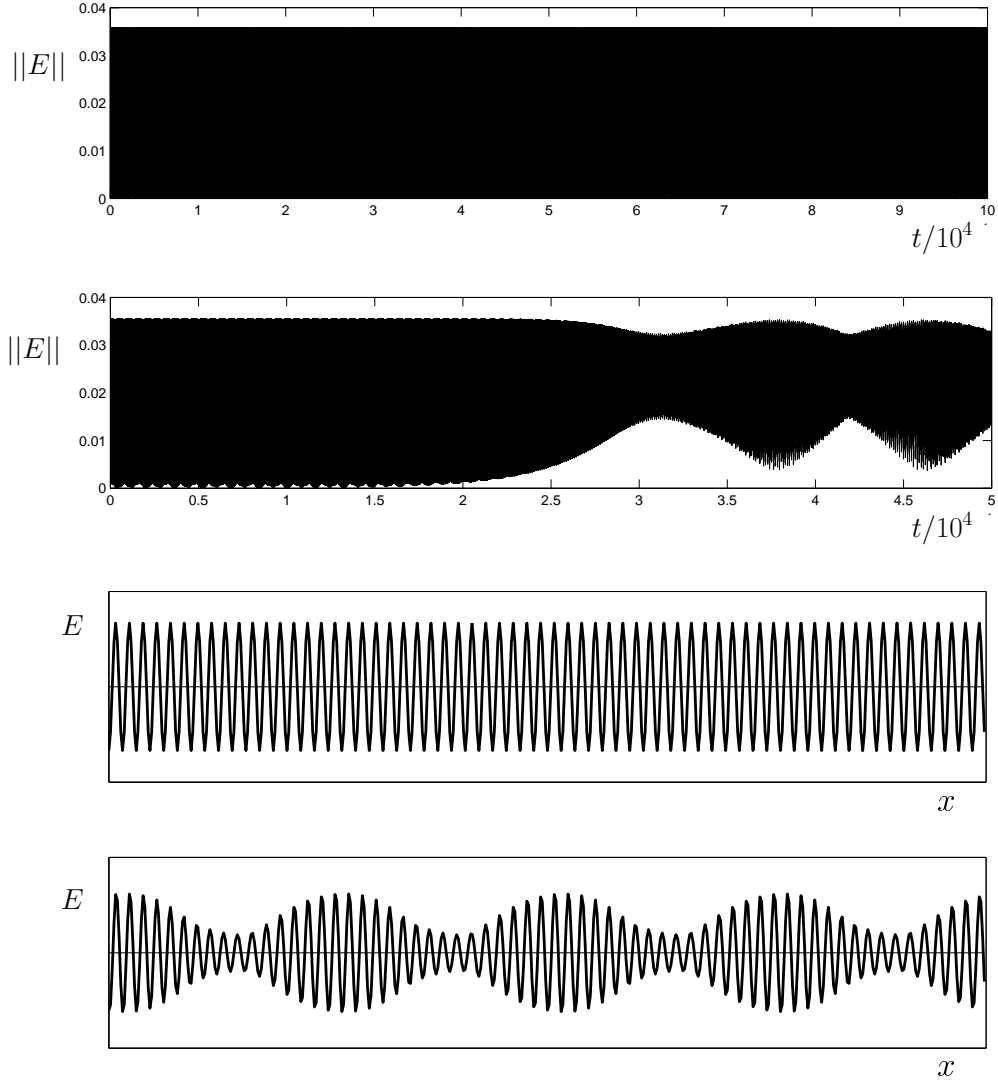


Figure 5: MLE simulation results starting from a CW ($\kappa = 1$, $\theta = \frac{\pi}{4}$ and $\rho^2 = 1$) with a 10^{-4} perturbation. From top to bottom: time evolution of the spatial norm of E for ω^+ and ω^- , spatial profile of E at $t = 75000$ and ω^+ , and spatial profile of E at $t = 30000$ for ω^- .

by the Universidad Politécnica de Madrid (R05/11071).

-
- [1] H. Winful and G. Cooperman, Appl. Phys. Lett. **40**, 298 (1982).
 - [2] C. de Sterke and J. Sipe, Progress in Optics **XXXIII**, 203 (1994).
 - [3] C. de Sterke, J. Opt. Soc. Am. B **15**, 2660 (1998).
 - [4] A. Aceves, CHAOS **10**, 584 (2000).

- [5] R. Goodman, M. Weinstein, and P. Holmes, *J. Nonlinear Sci.* **11**, 123 (2001).
- [6] A. Yulin and D. Skryabin, *Phys. Rev. E* **67**, 023611 (2003).
- [7] H. Sakaguchi and B. Malomed, *J. Phys. B: At. Mol. Opt. Phys.* **37**, 1443 (2004).
- [8] C. Martel, *CHAOS* **15**, 013701 (2005).
- [9] C. Martel, J. Vega, and E. Knoboch, *Physica D* **174**, 198 (2003).
- [10] C. Martel and J. Vega, *Nonlinearity* **9**, 1129 (1996).
- [11] C. Martel and J. Vega, *Nonlinearity* **11**, 105 (1998).
- [12] G. P. Agrawal, *Nonlinear Fiber Optics*, Optics and Photonics (Academic Press, 1995).
- [13] T. K. W. Lauterborn and M. Weisenfeld, *Coherent Optics: Fundamentals and Applications* (Springer Verlag, 1993).
- [14] G. M. W. M.P. Sørensen, M. Brio and J. Moloney, *Physica D* **170**, 287 (2002).
- [15] M. Cross and P. Hohenberg, *Rev. Mod. Phys.* **65**, 851 (1993).
- [16] J. Lambert, *Numerical Methods for Ordinary Differential Systems: The Initial Value Problem* (John Wiley and Sons, 1995).
- [17] C. Canuto, H. Hussani, A. Quarteroni, and T. Zang, *Spectral Methods in Fluid Mechanics*, Springer Series in Computational Physics (Springer-Verlag, 1988).
- [18] M. Frigo and S. Johnson, *FFTW* (available at <http://www.fftw.org> , 2004).